

On the response of Southern Ocean water-masses to atmospheric meridional moisture advection

Oleg A. Saenko

School of Earth and Ocean Sciences, University of Victoria, Victoria, BC, Canada

Matthew H. England

Centre for Environmental Modelling and Prediction, University of New South Wales, Sydney, NSW, Australia

Received 24 October 2002; revised 2 January 2003; accepted 5 March 2003; published 25 April 2003.

[1] We investigate the role of atmospheric moisture advection in determining Southern Ocean water-mass properties in a coupled climate model. Two sensitivity experiments are presented in which the winds advecting moisture are either reduced or enhanced south of 45°S. It is shown that a variation in meridional winds in the Southern Ocean can generate large anomalies of subsurface potential temperature (T) and salinity (S). A reduction (increase) in southward atmospheric moisture advection tends to be balanced by a corresponding reduction (increase) in northward freshwater transport in Antarctic Intermediate Water. The response of both T and S is larger in the case of reduced southward moisture advection, as this corresponds to an overall reduction of Southern Ocean stratification. The interior ocean T – S response is not always density-compensating, particularly in the Indian and Pacific Oceans. This is unlike zonal wind variations which have a tendency to change T – S in a density-conserving manner. Our study suggests that variability in meridional winds over the Southern Ocean can alter local water-mass formation rates significantly.

INDEX TERMS: 4207 Oceanography: General: Arctic and Antarctic oceanography; 4283 Oceanography: General: Water masses; 4504 Oceanography: Physical: Air/sea interactions (0312); 4532 Oceanography: Physical: General circulation. **Citation:** Saenko, O. A., and M. H. England, On the response of Southern Ocean water-masses to atmospheric meridional moisture advection, *Geophys. Res. Lett.*, 30(8), 1433, doi:10.1029/2002GL016516, 2003.

1. Introduction

[2] Several recent studies have investigated the role of the zonal wind stress in determining the thermohaline properties of Antarctic Intermediate Water (AAIW) and Subantarctic Mode Water (SAMW). *Ribbe* [1999, 2001] used a series of ocean model experiments to show how an increased zonal wind stress over the Southern Ocean can drive a more pronounced salinity minimum at intermediate depths. The increased zonal wind stress forces a stronger northward flow of Antarctic and Subantarctic waters in the Ekman layer. *Rintoul and England* [2002] used direct observations and a coupled climate model to show how significant, density-compensating anomalies in SAMW potential temperature (T) and salinity (S) are controlled by variations in northward Ekman transport across the Subantarctic Front. *Saenko and Weaver* [2001] used an intermediate complexity coupled

climate model to illustrate the importance of wind stress at the air-sea ice interface for the process of AAIW formation.

[3] The above studies focus on the role of Southern Ocean winds in terms of passing momentum to either the ocean or sea-ice or both. Moreover, they mainly emphasised a zonal (eastward) component of wind stress, given its importance for the northward Ekman transport of both water and sea-ice. The role of *meridional* winds in generating T – S anomalies in the subsurface Southern Ocean has hitherto not been investigated.

[4] While meridional winds determine local east-west Ekman transport (negligible compared to the net Antarctic Circumpolar Current (ACC) transport), they can also influence the ocean via their capacity to transport moisture in the troposphere. At steady state, net poleward atmospheric moisture transport must be balanced by net equatorward transport of fresh water in the ocean. Thus, one may expect variations of meridional winds in the Southern Hemisphere to generate anomalies of ocean thermohaline properties, including those at the AAIW and SAMW depth range.

[5] Evidence for interannual-pentadal fluctuations in meridional Southern Ocean winds can be found in the pattern of variability associated with the Antarctic Circumpolar Wave (*White and Peterson* [1996]). In addition, longer-term trends in Southern Hemisphere sea-level pressure [*Fyfe et al.*, 1999], [*Boer et al.*, 2000] and atmospheric moisture content [*Boer*, 1995] are likely to be a consequence of enhanced atmospheric greenhouse gases over the next 10–100 years. Poleward transport of moisture generally increases in the warmer climate as a consequence of increased moisture content in the warmer atmosphere [*Boer*, 1995]. Thus, for both variability and longer-term change, it is important that we understand the likely oceanic response to changes in Southern Ocean meridional winds and moisture advection.

[6] The largest contribution to the net moisture convergence from winds is in the tropics. However, winds also play an important role in transporting moisture to middle and high latitudes, including in the Southern Ocean (Figure 1). The goal of this note is to illustrate the effect of the latter on ocean thermohaline properties using the results of two sensitivity experiments in a coupled climate model.

2. The Model and Design of Experiments

[7] The coupled model we use comprises an ocean GCM [*Pacanowski*, 1996], an energy-moisture balance atmosphere model [*Weaver et al.*, 2001] and a dynamic - thermodynamic sea ice model [*Bitz et al.*, 2001]. The coupled model is described in detail in *Weaver et al.* [2001]. All

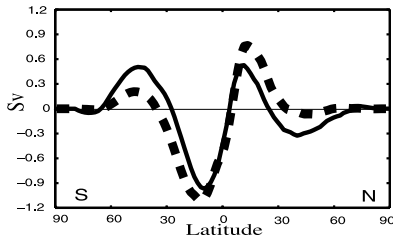


Figure 1. Northward oceanic freshwater transport or net southward atmospheric moisture transport (solid) and advective component of the southward atmospheric moisture transport (dashed), simulated by the model at steady state (CTR).

model components have the same horizontal resolution of $3.6^\circ \times 1.8^\circ$ in longitude and latitude, respectively. The ocean model uses isopycnal mixing after *Gent and McWilliams* [1990] with the coefficients of thickness diffusivity and isopycnal diffusivity set to $1.0 \times 10^3 \text{ m}^2 \text{ s}^{-1}$ and $2.0 \times 10^3 \text{ m}^2 \text{ s}^{-1}$, respectively. The horizontal tracer advection is accomplished using a flux-corrected transport scheme. The vertical diffusivity in the model follows the profile of *Bryan and Lewis* [1979], with values ranging from $6 \times 10^{-5} \text{ m}^2 \text{ s}^{-1}$ in the upper ocean to $1.6 \times 10^{-4} \text{ m}^2 \text{ s}^{-1}$ in the deep ocean. There are 19 vertical levels in the ocean model that vary smoothly in thickness from 50 m at the surface to 518 m at the deepest level.

[8] The atmospheric model does not calculate winds and wind stress. These are prescribed from the NCEP/NCAR reanalysis [*Kalnay et al.*, 1996], averaged over the period 1958–1997 to form an annual cycle from the monthly fields. However, the model does calculate surface heat and freshwater fluxes, as well as the atmospheric transport of sensible heat and moisture. Of importance here is our use of the model version in which the moisture transport is accomplished by means of both diffusion and advection (see *Weaver et al.* [2001] for details).

[9] The model was first spun up for several thousand years to a steady state. The final year of this spin-up was subsequently used as a control state (CTR) and also as an initial condition for two sensitivity experiments. In the sensitivity experiments, we multiply the meridional component of the winds advecting moisture by either a factor of 1.5 (ME1.5 experiment) or a factor of 0.5 (ME0.5 experiment) south of 45°S . The two sensitivity experiments were run for a period of 100 years, sufficient for equilibration of the intermediate layers. It should be noted that the wind stress was not perturbed in the ME1.5 and ME0.5 experiments, allowing us to isolate moisture advection effects from other forcings. Thus, the only difference between the three model experiments is the meridional moisture advection south of 45°S .

3. Results

[10] Meridional moisture advection (MA) is given by the product of specific air humidity (q) and meridional wind speed (v). South of 30°S contours of air humidity are predominantly zonal, with q decreasing poleward due to a strong dependence of saturation humidity on air temperature (Figure 2, upper panel). In addition, the large-scale pattern of winds in the Southern Ocean is predominantly zonal.

Thus, values of qv are relatively small at high southern latitudes (for a zonal integral in CTR see Figure 1). However, between 45°S – 55°S and 100°E – 150°E a combination of relatively strong meridional winds and high values of humidity creates an enhanced southward moisture advection (up to $15 \times 10^{-3} \text{ m s}^{-1}$, Figure 2 lower panel). Elsewhere at 45°S – 55°S , qv is more typically $8 \times 10^{-3} \text{ m s}^{-1}$.

[11] Variations in the meridional MA are able to generate considerable anomalies of T and S in the subsurface Southern Ocean. Zonally-averaged sections of the T – S response to MA changes are shown in Figure 3. As is the case in most modelling studies, this T – S analysis is performed on fixed depth levels, not isopycnals, so can include “heave” effects (*Bindoff and McDougall* [1994]). The largest anomalies of S penetrate into the subsurface ocean, roughly following the salinity minimum associated with AAIW. In response to an increased (reduced) southward MA, AAIW becomes fresher (saltier), tending to maintain a balance between the net southward moisture transport in the atmosphere and the net northward freshwater transport in the ocean (Figure 3). It is worth noting that heave effects are relatively minor, mainly because the wind-stress remains constant across experiments, so that Ekman pumping is unchanged. Specifically, heave effects contribute only about 5–15% of the T – S changes simulated in the ME0.5 and ME1.5 experiments (Figure not shown).

[12] With increased southward MA in the ME1.5 experiment, the upper ocean south of 60°S becomes fresher, making the water column more stratified and in turn the subsurface ocean warmer (Figure 3). In contrast, reduced southward MA in the ME0.5 experiment increases surface salinity and therefore decreases the stratification in the Southern Ocean. Significant subsurface cooling results, penetrating beyond 1500-m depth (Figure 3). The cold water which creates these negative T anomalies originates from a localized region of enhanced downwelling adjacent to the Antarctic coast, located near the longitudes of enhanced southward MA (around 110°E). In that region,

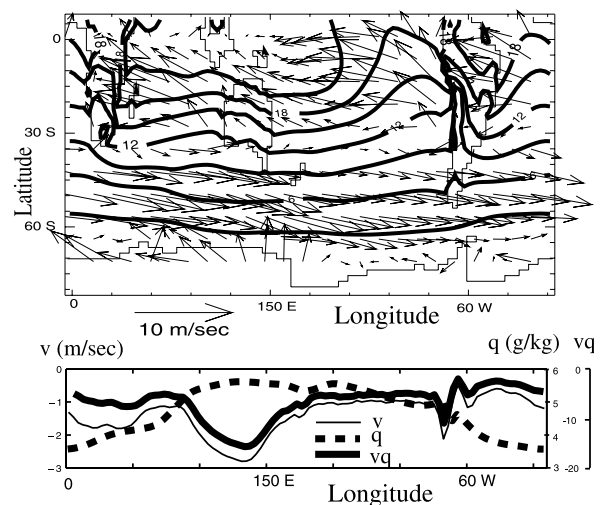


Figure 2. Annually-averaged specific humidity (g/kg) and near-surface wind field (upper panel) and average meridional component of the wind (v), specific humidity (q) and the product of v and q between 45°S and 55°S (lower panel). Quantities shown are those diagnosed in the CTR experiment. Units of moisture transport (qv) are $10^{-3} \text{ m sec}^{-1}$.

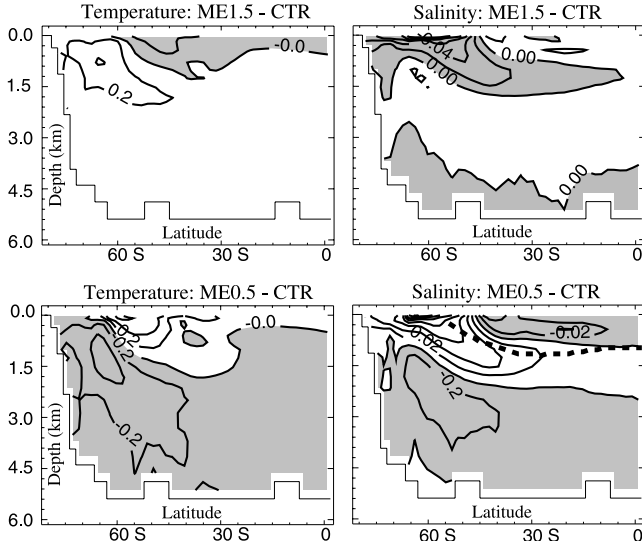


Figure 3. Sections of differences between ME1.5 and CTR (top) and between ME0.5 and CTR (bottom) of annually and zonally averaged potential temperature ($^{\circ}\text{C}$) and salinity (psu). Negative values are shaded. The dashed curve in the lower right panel indicates the depth of the 27.3 kg/m^3 density surface in CTR.

the reduction of southward atmospheric moisture flux increases the surface salinity by as much as 0.7 psu . This destabilizes the water column and favours downwelling and convection, resulting in heat release from the subsurface ocean. The latter in turn reduces the local sea-ice coverage. This increases heat loss by the ocean, warming up the local near-surface air by as much as 2°C on the annual mean (Figure not shown). In this manner, changes in the atmospheric MA can result in significant air-temperature changes via an ocean circulation and sea-ice feedback.

[13] The reduction of southward MA and associated decrease of Southern Ocean stratification in the ME0.5 experiment results in T and S root-mean-square (RMS) differences of, respectively, 0.51°C and 0.06 psu within the AAIW potential density range ($27.0 < \sigma_t < 27.7$). The corresponding T and S RMS differences in the ME1.5 experiment (compared to CTR) are 0.25°C and 0.04 psu . Hence, the reduction of southward moisture transport and the associated reduction of Southern Ocean stratification in ME0.5 leads to larger subsurface thermohaline changes than when moisture advection (and stratification) is increased.

[14] Water-mass formation rates are controlled largely by surface density properties. It is of interest then to assess changes in surface layer density in the MA sensitivity runs. The surface RMS density difference between ME0.5 and CTR is 0.10 kg/m^3 within the AAIW potential density range, with a tendency for increased density as moisture advection decreases. This drives a more rapid AAIW subduction than in CTR. The converse holds for ME1.5, with a tendency for freshening of the surface layer (the RMS density difference is 0.09 kg/m^3). In both experiments then, changes to the meridional MA drive significant changes in upper layer density, thereby altering local water-mass formation rates.

[15] The above analyses of zonal mean and RMS $T-S$ and density differences alias some structure in the intermediate water region. In particular, the magnitude of $T-S$ response differs considerably between ocean basins, with the largest changes in the Indian and Pacific sectors (Figure 4). Importantly, the $T-S$ response to changes in meridional MA is not always density-compensating. This is particularly the case in the Indian Ocean sector, where the scatter of $T-S$ response is largest. There, a significant volume of AAIW sees a transformation in density in excess of 0.05 kg/m^3 (36% of total AAIW volume in ME0.5 and 20% in ME1.5). The scatter plot of $T-S$ difference shows that for the most part AAIW becomes fresher in ME1.5 and more saline in ME0.5. However, the response in T varies between regions and experiments. The most significant AAIW density change is seen in the Indian Ocean in ME0.5, with 37% of total AAIW volume cooling and becoming more saline (the lower right quadrant of Figure 4a). In this run, AAIW density can increase by up to 0.25 kg/m^3 . This suggests that variability in meridional moisture transport over the Southern Ocean is capable of altering subsurface water-mass properties significantly.

[16] The large scattering of $T-S$ response in the Indian Ocean sector appears to be due in part to a steering effect of the ACC around the Kerguelen Plateau (near 80°E). This affects the temperature structure more than the salinity (Figure 5), which explains the large density response in the Indian Ocean sector. Enhanced southward moisture advection near these longitudes (Figure 2, lower panel) also plays a role, but more in setting a magnitude, rather than a dipole-like structure of T response along the ACC (Figure 5a). This structure is coherent over the water column from the surface down to intermediate depths in both experiments. It thus appears that north-south topographic steering of the ACC can affect the propagation of high latitude T anomalies into the interior. Whilst the salinity response is found to be more

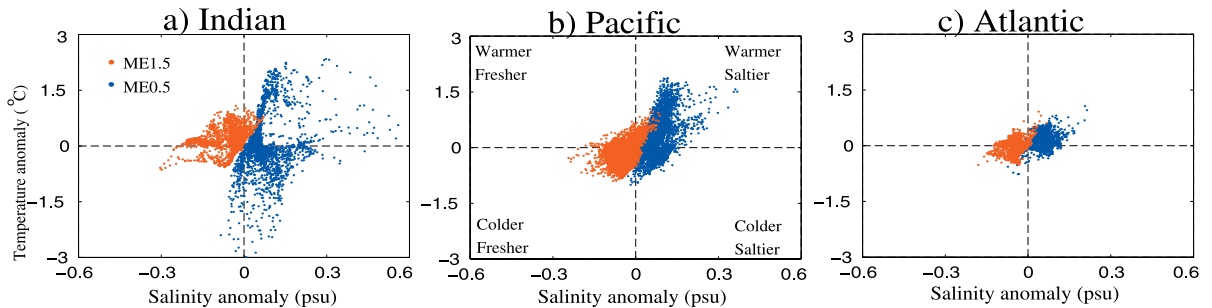


Figure 4. Scatter plot of $T-S$ differences between ME1.5 and CTR (red) and ME0.5 and CTR (blue) for the potential density range of $27.0\text{--}27.7 \text{ kg/m}^3$ south of 30°S in the three oceans: (a) Indian, (b) Pacific and (c) Atlantic. This analysis of $T-S$ change is performed on pressure surfaces, though as described in the text, heave effects are minimal.

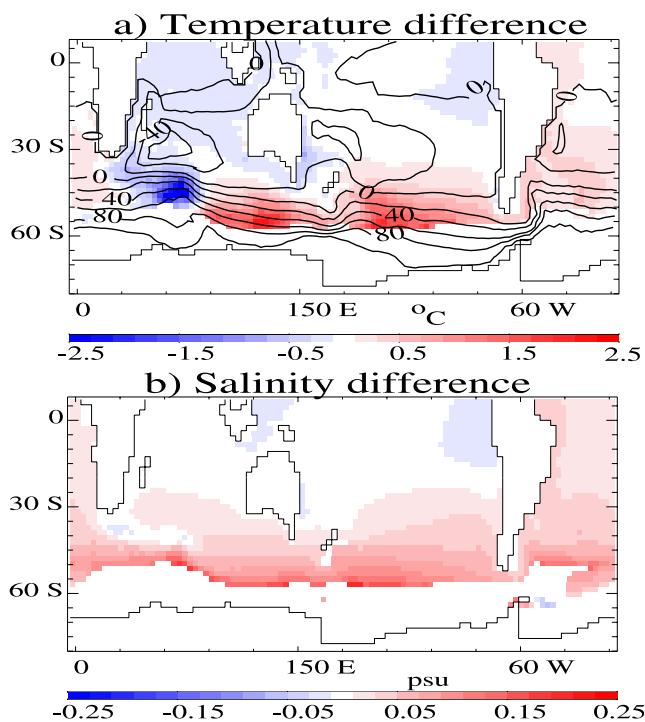


Figure 5. Differenced fields of (a) potential temperature, and (b) salinity between ME0.5 and CTR following the 27.3 kg/m^3 potential density surface. Overplotted in (a) are contours of the CTR barotropic streamfunction. The zonal-mean depth of the 27.3 kg/m^3 potential density surface in CTR is indicated in Figure 3.

uniformly distributed along the ACC, it penetrates deepest in the south-east Pacific Ocean. This is a region of enhanced formation of AAIW and SAMW [McCartney, 1977], [England *et al.*, 1993].

4. Conclusions

[17] Using a coupled model we have described the response of Southern Ocean water-mass properties to variations of meridional moisture advection south of 45°S . It should be noted that the MA variations can be due to either changes in meridional winds, or changes in atmospheric moisture, or indeed a combination of the two. The response of subsurface $T-S$ is larger in the case of reduced southward moisture advection, which corresponds to an overall reduction of stratification in the Southern Ocean. The decrease (increase) of southward moisture advection in the atmosphere tends to be balanced in the ocean by a decrease (increase) of northward freshwater transport, making AAIW saltier (fresher).

[18] The sensitivity of our coupled climate model to changes in meridional moisture advection appears largest in the Indian and Pacific sectors, where the AAIW response shows significant $T-S$ transformations and associated change in density. Our study suggests that a substantial freshening of AAIW can be forced by an increase in meridional moisture advection over the Southern Ocean. This result may have relevance to the interpretation of the large-scale freshening of intermediate waters that has been observed recently in the Indian and Pacific Oceans (see, e.g., Wong *et al.* [1999], Banks *et al.* [2000]).

[19] We conclude that variations of the meridional component of winds at mid-latitudes of the Southern Hemisphere can generate significant anomalies in Southern Ocean $T-S$, particularly at the depth range of AAIW and SAMW, by affecting meridional moisture transport. Previous studies have had a tendency to focus on the zonal wind stress as the key component of the wind's driving force in establishing subsurface $T-S$ patterns in the Southern Ocean. Other effects due to the winds are also possible. Here we have illustrated the water-mass response to changes in meridional winds via their capacity to transport moisture.

[20] **Acknowledgments.** This research was supported in part by the Canadian Climate Change Action Fund and in part by the Australian Research Council. We would like to thank E. Wiebe for assistance.

References

- Banks, H. T., R. A. Wood, J. M. Gregory, T. C. Johns, and G. S. Jones, Are observed decadal changes in intermediate water masses a signature of anthropogenic climate change?, *Geophys. Res. Lett.*, **27**, 2961–2964, 2000.
- Bindoff, N. L., and T. J. McDougall, Diagnosing climate change and ocean ventilation using hydrographic data, *J. Phys. Oceanogr.*, **24**, 1137–1152, 1994.
- Bitz, C. M., M. M. Holland, A. J. Weaver, and M. Eby, Simulating the ice-thickness distribution in a coupled climate model, *J. Geophys. Res.*, **106**, 2441–2464, 2001.
- Boer, G. J., Some dynamical consequences of greenhouse gas warming, *Atmos-Ocean*, **33**, 731–751, 1995.
- Boer, G. J., G. Flato, and D. Ramsden, A transient climate change simulation with greenhouse gas and aerosol forcing: projected climate to the twenty-first century, *Clim. Dyn.*, **16**, 427–450, 2000.
- Bryan, K., and L. Lewis, A water mass model of the world ocean, *J. Geophys. Res.*, **84**, 311–337, 1979.
- England, M. H., J. S. Godfrey, A. C. Hirst, and M. Tomczak, The mechanism for Antarctic Intermediate Water renewal in a world ocean model, *J. Phys. Oceanogr.*, **23**, 1553–1560, 1993.
- Fyfe, J. C., G. J. Boer, and G. M. Flato, The Arctic and Antarctic Oscillations and their projected changes under global warming, *Geophys. Res. Lett.*, **26**, 1601–1604, 1999.
- Gent, P. R., and J. C. McWilliams, Isopycnal mixing in ocean general circulation models, *J. Phys. Oceanogr.*, **20**, 150–155, 1990.
- Kalnay, E., M. Kanamitsu, and R. D. W. Kistler *et al.*, The NCEP/NCAR 40 year reanalysis project, *Bull. Amer. Meteorol. Soc.*, **77**, 437–471, 1996.
- McCartney, M. S., Subantarctic mode water, in *A Voyage of Discovery*, edited by M. Angel, *Deep-Sea Res.*, **24**, (Suppl.), 103–119, 1977.
- Pacanowski, R., *MOM 2 Documentation, user's guide and reference manual*, GFDL Ocean Group Tech. Rep. 3, GFDL, Princeton, NJ., pp. 329, 1996.
- Ribbe, J., On wind-driven mid-latitude convection in ocean general circulation models, *Tellus*, **51A**, 517–525, 1999.
- Ribbe, J., Intermediate Water Mass production controlled by southern hemisphere winds, *Geophys. Res. Lett.*, **28**, 535–538, 2001.
- Rintoul, S. R., and M. H. England, Ekman transport dominates local air-sea fluxes in driving variability of Subantarctic Mode Water, *J. Phys. Oceanogr.*, **32**, 1308–1321, 2002.
- Saenko, O. A., and A. J. Weaver, Importance of wind-driven sea ice motion for the formation of Antarctic Intermediate Water, *Geophys. Res. Lett.*, **28**, 4147–4150, 2001.
- Weaver, A. J., M. Eby, and E. C. Wiebe *et al.*, The UVic Earth System Climate Model: Model description, climatology and application to past, present and future climates, *Atmosphere-Ocean*, **39**, 361–428, 2001.
- White, W. B., and R. Peterson, An Antarctic Circumpolar Wave in surface pressure, wind, temperature and sea ice extent, *Nature*, **380**, 699–702, 1996.
- Wong, A. P. S., N. L. Bindoff, and J. A. Church, Large-scale freshening of intermediate waters in the Pacific and Indian Ocean, *Nature*, **400**, 440–443, 1999.

O. A. Saenko, School of Earth and Ocean Sciences, University of Victoria, PO Box 3055, Victoria, BC V8W 3P6, Canada. (oleg@ocean.seos.uvic.ca)

M. H. England (corresponding author), Centre for Environmental Modelling and Prediction, School of Mathematics, University of New South Wales, Sydney, NSW 2052, Australia. (M.England@unsw.edu.au)